Feasibility study on the seismic isolation of pool-type LMFBR 3. Experiments of lead and elastomeric bearings

A.Yasaka, M.Iizuka, Y.Fukushima & Y.Hirao
Kajima Corporation, Tokyo, Japan
Y.Sonoda & M.Kurihara
Hitachi Ltd, Tokyo, Japan

1. INTRODUCTION

The seismic base isolation systems are very efficient in protecting important internal equipments as well as buildings from earthquake vibration. Many advantages can be anticipated when this system is applied to the most important (in seismic rating) structures such as the FBR plant. The base isolation system composed of laminated rubber bearings and a certain kind of energy dissipators are considered to be the most practical at present. The lead and elastomeric bearing, which has been developed in New Zealand, is a laminated rubber bearing with a lead plug down its center. It provides the combined features of horizontal flexibility and energy absorption capability in a single unit. In order to investigate the feasibility of adopting the lead and elastomeric bearings to the seismic isolation systems of the pool type LMFBR plants, loading tests and shaking table tests were conducted. This paper describes the experimental results of the mechanical behavior and vibration characteristics.

2. LOADING TESTS

2.1 Specimens and testing apparatus

The test specimens are shown in Figure 1a. The specimens were designed to support the dead weight, W of 100tf and to have bilinear hysteretic loop parameters of elastic stiffness K1 = 0.1W/cm = 10tf/cm (f1 = 1.6 Hz), post-yield stiffness K2 = 0.01W/cm = 1tf/cm (f2 = 0.5 Hz) and yield force F = 0.05W = 5tf. These values were determined from the results of the earthquake and wind response analyses. Two methods of mounting details were adopted. One was the mounting by dowels, and the other by bolts. In the dowel type, 4 dowels on the flange plate were tailed in mortises of the bearing. In the bolt type, the flange plates were fixed to the bearing by bolts. The other details were the same with each other. The material used in the specimens were natural rubber (durometer hardness : 57, shear modulus : 8.1 Kgf/cm2) and lead of high purity.

Testing apparatus is shown in Figure 1b. Both shear force and axial force were provided by the actuators. A special link apparatus was used to constrain the specimens to deform in pure shear.

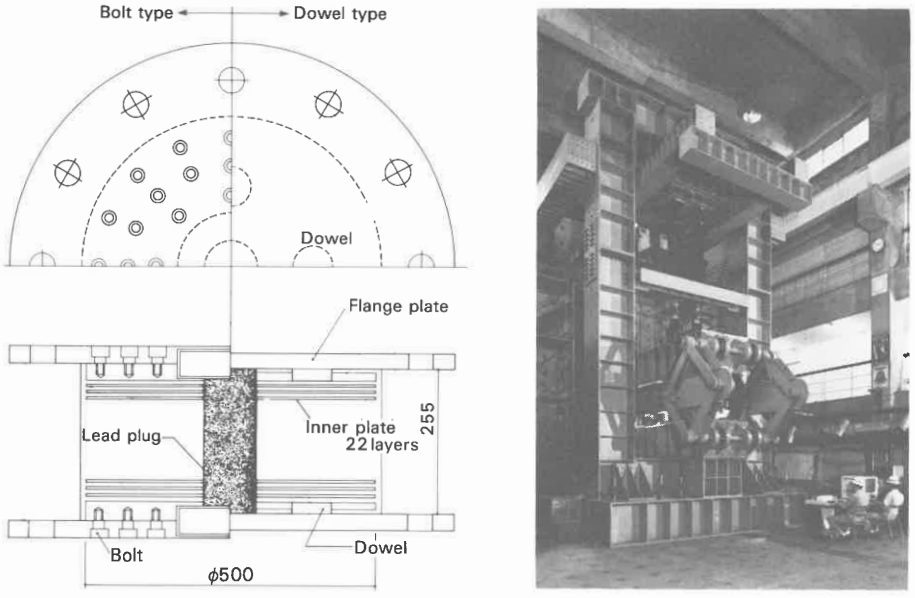

Figure 1. Specimen (right side: dowel type, left side: bolt type) (a); testing apparatus (b)

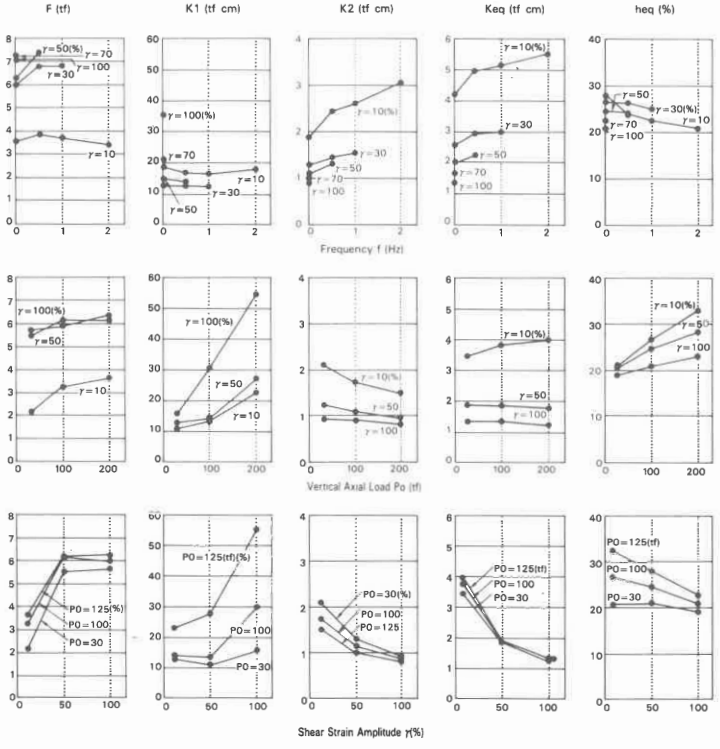

Figure 2. Effect of frequency f, vertical axial load Po and shear strain amplitude γ on hysteretic loop parameters.

2.2 Test results

In order to investigate the shear hysteretic characteristics, the specimens were dynamically loaded under constant axial load Po, shear strain amplitude $\pm\gamma$ ($\gamma = \delta H/h$; δH: horizontal displacement, h : effective elastomer height) and frequency f. Five hysteretic loop parameters of K1 (elastic stiffness), K2 (post-yield stiffness), F (yield force), Keq (equivalent stiffness) and heq (equivalent viscous damping factor) were determined from the load-deflection curves obtained by the tests. The relationships between these hysteretic loop parameters and loading conditions are shown in Figure 2. All of the hysteretic loop parameters were influenced by the shear strain amplitudes, and K1 and heq by axial loads. K2, Keq and heq in the small deformation range were affected by frequencies.

Shear fatigue tests were conducted. Cyclic shear loadings were applied to the specimens under Po = 100tf, γ = 50%, and f = 0.5 Hz. Loadings were repeated 8 times at intervals of 30 minutes. One set of loading was composed of ten cycles. The results of the 1st loading and the 8th loading are shown in Figure 3. In a set of serial cyclic loadings, restoring force gradually decreased, but with a time interval of 30 minutes, the properties recovered to the initial state.

Static shear tests for large deformation were carried out. Both types of the specimens could deform more than 200% shear strain bearing the axial load of 100tf without any damages. Test results are shown in Figure 4a. In the large deformation range, the restoring force characteristics were greatly affected by the mounting details.

Static pure tension test was conducted. Test results are shown in Figure 4b. The specimen failed at the rubber layer, when elongation ε ($\varepsilon = \delta v/h$; δv:tensile displacement, h : effective elastomer height) reached 165%.

3. SHAKING TABLE TESTS

3.1 Specimen and earthquake input

A specimen used in the shaking table tests is shown in Figure 5a. The specimen is a scale model of a trial design model of a LMFBR plant. The specimen was designed to have the dynamic properties which were simulated to those possessed by a full scale model, on the basis of the similarity method. The specimen is a steel frame model with four-story and one-bay, which was mounted on four sets of 4tf bearings. The 4tf bearing is a scale model of a 500tf bearing which is applied in the trial design model. Therefore, the time scale factor is approximately $\sqrt{11}$. Two kinds of properties for the 500tf bearing were taken into account. They were different in the yield level α only, as follows.

1) Elastic stiffness : K1 = 0.04W/cm = 20tf/cm (f1 = 1.0Hz)
   Post-yield stiffness : K2 = 0.01W/cm = 5tf/cm (f2 = 0.5Hz)
   Yield force : F = 0.05W = 25tf (α = F/W = 0.05)
2) K1 and K2 are the same as above. F = 0.025W = 12.5tf (α = 0.025)

where W is supporting load of 500tf. These values were determined in consideration to the floor response spectrum. These properties were scaled down to those of 4tf bearing using the similarity method.

Two input earthquake motions were the El Centro 1940 NS component and an artificial earthquake motion. In generating the artificial earthquake motion, its frequency properties were determined in consideration to the fundamental natural frequency of the base isolation system.

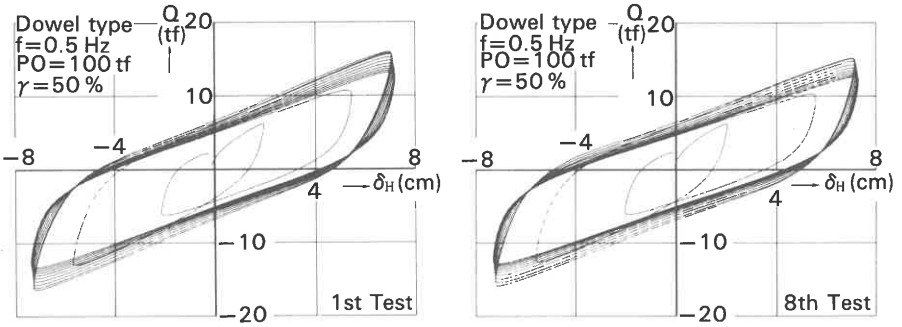

Figure 3. Shear force (Q) - horizontal displacement (δH) curves obtained by shear fatigue tests.

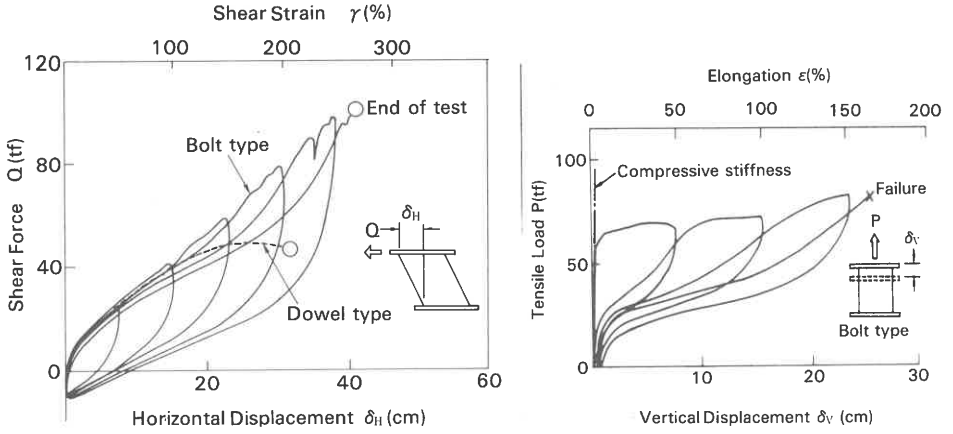

Figure 4. Restoring force characteristics in shear (a) and in pure tension (b).

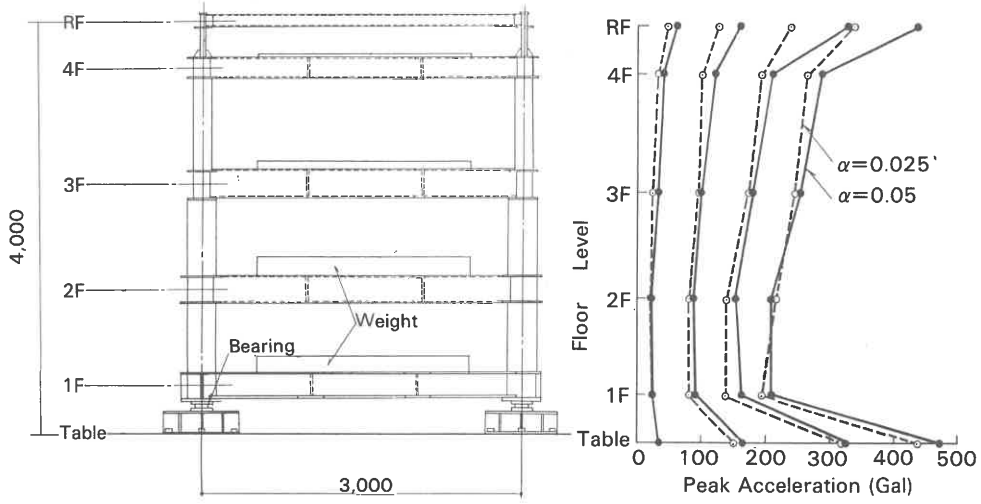

Figure 5. Specimen used in shaking table tests (a) ; peak response acceleration (b).

3.2 Test results

The test results for the artificial earthquake input are described hereunder. The results of the El Centro input were similar.

The peak response accelerations are shown in Figure 5b. The relationship between the relative displacement in the isolation story and the peak table acceleration is shown in Figure 6a, and the floor response spectra in Figure 6b. As shown in Figure 5b, the peak response accelerations were roughly constant with height and less than the peak table accelerations. And the lower yield level (smaller α) showed slightly lower acceleration responses. But, as shown in Figure 6a, the lower yield level showed slightly larger displacement responses. The floor response spectrum at the 2nd floor, where the reactor vessel is supported, was not influenced much by the yield level. But, as shown in the spectrum at the 4th floor, the lower yield level reduced the floor response spectrum in the short-period range.

3.3 Simulation analysis

Simulation analyses were performed to confirm that the analytical method was appropriate. The steel frame was represented by 5 lumped masses, and the isolation story was modeled as rocking and swaying springs. The swaying spring was assumed as the bilinear hysteretic spring which simulated the load - deflection curves of the isolation story obtained by the static loading tests.

Examples of the analytical results are shown in Figure 7. It can be seen that both calculated acceleration time history and calculated floor response spectrum agree well with the observed results.

4. CONCLUSION

The effectiveness of the lead and elastomeric bearings has been demonstrated by the tests. In the loading tests, the effect of the shear displacement amplitude, the axial load and the frequency on the shear hysteretic characteristics were quantified. And it was confirmed that the mounting details remarkably influenced the restoring force characteristics in the large deformation range. Furthermore, it was demonstrated that lead and elastomeric bearings had good fatigue properties, and they had sufficient ductilities in both shear and tension. From the shaking table tests, it was demonstrated that the peak response accelerations were greatly reduced. The effect of the yield level of the bearing on the responses was examined. And from the simulation analyses, it was recognized that the analytical method was reasonable.

It can be concluded that the lead and elastomeric bearings are very feasible devices to apply to the seismic base isolation systems of LMFBR plants, in view of both the mechanical performance and the vibration behavior.

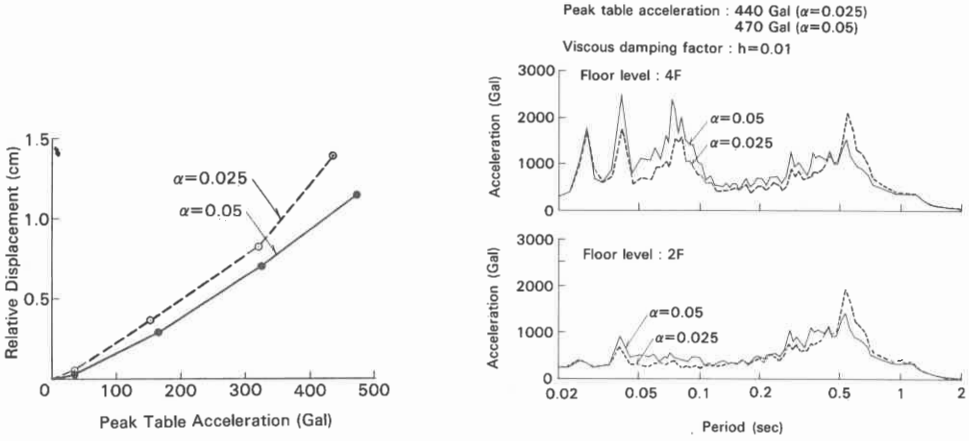

Figure 6. Relationship between relative displacement and peak table acceleration (a) ; effect of yield level on floor response spectrum (b).

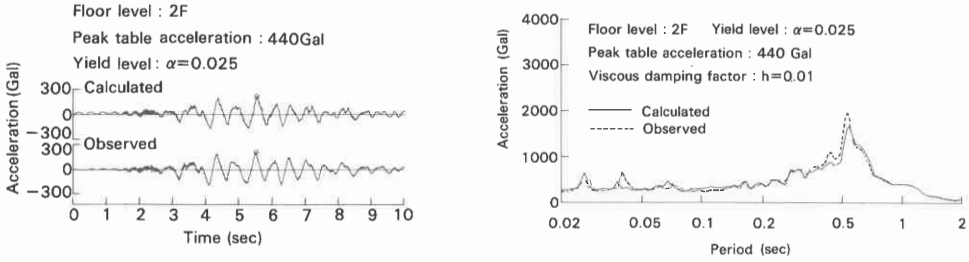

Figure 7. Comparison of calculated results and observed results in acceleration time history (a) and in floor response spectrum (b).

REFERENCES

Iizuka, M., Takabayashi, K., Yasaka, A., & Kurihara, M. 1986. Feasibility study of a seismic isolation system for fast breeder reactor plants. Proc. of the 7th Japan earthquake engineering symposium:1663-1668.

Robinson, W.H. 1982. Lead-rubber hysteretic bearings suitable for protecting structures during earthquakes. Earthquake Engineering and Structural Dynamics. 10:593-604.

Tyler, R.G. & Robinson, W.H. 1984. High-strain tests on lead-rubber bearings for earthquake loadings. Bulletin of the New Zealand National Society for Earthquake Engineering. 17.2:90-105.

Kelly, J.M. & Hodder, S.B. 1982. Experimental study of lead and elastomeric dampers for base isolation systems in laminated neoprene bearings. Bulletine of the New Zealand National Society for Earthquake Engineering. 15.2:53-67.